International Journal of Pharmaceutics 612 (2022) 121380

Contents lists available at ScienceDirect

International Journal of Pharmaceutics

journal homepage: www.elsevier.com/locate/ijpharm

# Antagonist G-targeted liposomes for improved delivery of anticancer drugs in small cell lung carcinoma

Manuela Carvalheiro [a,b,*], Margarida Ferreira-Silva [a,c], Denys Holovanchuk [a,c], H. Susana Marinho [c,d], João Nuno Moreira [e,f], Helena Soares [d,g], M. Luisa Corvo [a,b,*], Maria Eugénia M. Cruz [a]

[a] Instituto de Investigação do Medicamento (iMed.ULisboa), Faculdade de Farmácia, Universidade de Lisboa, Avenida Professor Gama Pinto, 1649-003 Lisboa, Portugal
[b] Departamento de Farmácia, Farmacologia e Tecnologias em Saúde, Faculdade de Farmácia, Universidade de Lisboa, Avenida Professor Gama Pinto, 1649-003 Lisboa, Portugal
[c] Departamento de Química e Bioquímica, Faculdade de Ciências, Universidade de Lisboa, 1749-016 Lisboa, Portugal
[d] Centro de Química Estrutural, Faculdade de Ciências, Universidade de Lisboa, Campo Grande, 1749-016 Lisboa, Portugal
[e] CNC - Center for Neuroscience and Cell Biology, Center for Innovative Biomedicine and Biotechnology (CIBB), University of Coimbra, Faculty of Medicine (Polo 1), Rua Larga, 3004-504 Coimbra, Portugal
[f] UC – University of Coimbra, CIBB, Faculty of Pharmacy, Pólo das Ciências da Saúde, Azinhaga de Santa Comba, 3000-548 Coimbra, Portugal
[g] Escola Superior de Tecnologia da Saúde de Lisboa, Instituto Politécnico de Lisboa, 1990-096 Lisboa, Portugal

A B S T R A C T

Ligand-mediated targeted liposomes have the potential to increase therapeutic efficacy of anticancer drugs. This work aimed to evaluate the ability of antagonist G, a peptide targeting agent capable of blocking the action of multiple neuropeptides, to selectivity improve targeting and internalization of liposomal formulations (long circulating liposomes, LCL, and stabilized antisense lipid particles containing ionizable amino lipid, SALP) to H69 and H82 small cell lung carcinoma (SCLC) cell lines. Antagonist G-targeted LCL and SALP were prepared by two different methods (either by direct covalent linkage at activated PEG grafted onto the liposomal surface or by post-insertion of DSPE-PEG-antagonist-G-conjugates into pre-formed liposomes). Association of the liposomal formulations with target SCLC cells was studied by fluorescence microscopy using fluorescence-labelled liposomes and confirmed quantitatively with [$^3$H]-CHE-labelled liposomes. An antisense oligodeoxynucleotide against the overexpressed oncogene *c-myc*(*as(c-myc)*) was efficiently loaded into SALP formulations, the encapsulation efficiency decreased due to the inclusion of the targeting ligand. Also, liposome size was affected by *as(c-myc)* physical chemical properties. The amount of antagonist G linked to the surface of the liposomal formulations was dependent on the coupling method and lipid composition used. Covalent attachment of antagonist G increased liposomes cellular association and internalization via receptor-mediated and clathrin-dependent endocytosis, as assessed in SCLC cell lines. Biodistribution studies in healthy mice revealed a preferential lung accumulation of antagonist G–targeted SALP as compared to the non-targeted counterpart. Lung levels of the former were up to 3-fold higher 24 h after administration, highlighting their potential to be used as delivery vectors for SCLC treatment.

## 1. Introduction

According to the World Health Organization (WHO), cancer is a leading cause of death worldwide, accounting for an estimated 10 million deaths in 2020. Treatment of cancer often involves local surgery in combination with radiotherapy and/or anticancer drugs (chemotherapy and hormone therapies and, more recently, monoclonal antibodies and immune checkpoint inhibitors) (Falzone et al., 2018). The latter, since drugs are able to reach every organ in the body via the bloodstream, are used for the treatment of metastatic cancers (Chabner and Roberts, 2005; Perez-Herrero and Fernandez-Medarde, 2015). Most anticancer agents used in current conventional chemotherapeutic treatments lack specificity to tumour cells limiting the use of high-dose intensity therapy, due to severe systemic and organ toxicities (Brignole et al., 2003; Schirrmacher, 2019) and cause the development of multidrug resistance (Gottesman et al., 2016). The drug efficacy of anticancer drugs can be improved either by increasing the drug dose that reaches the diseased tissue and/or by decreasing the dose that reaches normal tissues (Allen, 2002).

Drug delivery systems (DDS) such as liposomes, polymeric and inorganic nanoparticles and drug conjugates are able to transport anticancer drugs, including low molecular weight drugs and

* Corresponding authors at: Instituto de Investigação do Medicamento (iMed.ULisboa), Faculdade de Farmácia, Universidade de Lisboa, Avenida Professor Gama Pinto, 1649-003 Lisboa, Portugal.
*E-mail address:* lcorvo@ff.ulisboa.pt (M.L. Corvo).

https://doi.org/10.1016/j.ijpharm.2021.121380
Received 6 July 2021; Received in revised form 19 November 2021; Accepted 9 December 2021
Available online 13 December 2021

macromolecules such as nucleic acids and proteins, so that they avoid normal tissues and accumulate at higher concentrations in tumours, allowing them to be less toxic and more effective than circulating drugs (Danhier et al., 2010; Patra et al., 2018; Perez-Herrero and Fernandez-Medarde, 2015). These DDS are also able to incorporate hydrophobic compounds, protect them from degradation, decrease renal clearance and subsequently increase their blood lifetime, allowing for a controlled release into the target cells. In particular, long circulating liposomal DDS (LCL), i.e., stealth liposomes sterically stabilized by conjugation to polymers such as polyethylene glycol (PEG) to the liposome surface, were shown to provide stable formulations with improved pharmacokinetics and delayed clearance. These LCL result in much longer circulation times and enable the passive targeting to tumour tissues by using the enhanced permeability and retention effect for preferential extravasation from tumour vessels (Allen and Cullis, 2013; Danhier et al., 2010). Moreover, the physicochemical properties of liposomes can be tailored by changing the lipid bilayer compositions, which allows to control their size, surface charge, and use in an appropriate and simple way, without additional chemical synthesis steps that are used for the preparation of other carriers, i.e., polymer conjugates (Perez-Herrero and Fernandez-Medarde, 2015). Besides the ability of passive targeting, stealth liposomes DDS can be modified to be more selective toward cancer cells through active targeting strategies. For that, in addition to PEG, the surface of liposomes can be further modified with specific ligands, e.g., carbohydrates, peptides, proteins, antibodies, aptamers and enzymes, targeting surface molecules expressed by cancer cells. In comparison to non-targeted liposomes, the therapeutic advantage of ligand-targeted liposomes containing an entrapped drug results from an increased distribution to target tissues with the increased receptor-mediated uptake of liposomes by the target cells (Allen and Cullis, 2013).

The choice of the specific targeting ligand is very important to maximize the therapeutic effect of the active agent. To generate effective ligand-mediated targeted liposomes the cellular receptor and its ligand should show properties making them adequate as a tumour-specific target (Danhier et al., 2010; Yingchoncharoen et al., 2016). Three important criteria for choosing a ligand and receptor for liposomal active targeting are: (a) a homogeneous overexpression of the chosen molecule/marker on the surface of all targeted cancer cells and absent expression on normal cells (b), that once the ligand binds to its receptor, the ligand-receptor complex is not released into the blood circulation and (c), that the ligand-receptor complex is internalized into the target cell after binding e.g. through receptor-mediated endocytosis of liposomes. Peptides, similarly, to antibodies, can be used as ligands to specifically target tumour cells, and have the advantage of being less expensive and complex than antibodies.

Small cell lung carcinoma (SCLC) is an extremely aggressive neoplasm, originating from the neuroendocrine tissue. Patients with SCLC succumb to their disease within a few months after diagnosis and are in desperate need of new treatments (Poirier et al., 2020). As SCLC is characterized by overexpression of the oncogene *c-myc* this oncogene can be a good target for gene-based therapy. SCLC cells secrete multiple neuropeptides growth factors whose receptor-mediated actions can be inhibited by several peptide antagonists (Langdon et al., 1992; Sethi et al., 1992). Antagonist G (H–Arg-DTrp-N$^{me}$Phe-DTrp-Leu-Met-$NH_2$) binds to a broad range of structurally unrelated neuropeptide receptors and competitively inhibits the binding of neuropeptides to their receptors on the cell surface (MacKinnon et al., 1999). Therefore, antagonist G is a good choice as a targeting ligand to be covalently linked to the surface of liposomal formulations to improve treatment of SCLC (Moreira et al., 2001). Moreira *et al.* (Moreira and Gaspar, 2004) reported the use of antagonist G, as a targeting agent for sterically stabilized liposomes containing doxorubicin or nucleic acids in the treatment of human SCLC (Moreira and Gaspar, 2004; Moreira et al., 2001; Moreira et al., 2002; Santos et al., 2010).

The aim of this work was to prepare targeted DDS using different liposomal formulations with antagonist G as a ligand to specifically target SCLC cells and with the capacity to be internalized into those cells. We prepared antagonist G-targeted long circulating liposomes (LCL) able to carry both hydrophilic and hydrophobic low molecular weight molecules. We also prepared an antagonist G-targeted liposomal formulation containing an ionizable amino lipid (SALP) which was especially designed to encapsulate a negatively charged anticancer genetic drug the antisense oligodeoxynucleotide (asODN) against the oncogene c-myc. To study the internalization potential of both antagonist G-targeted formulations two different methods were used to attach the antagonist G onto the liposomal surface (direct covalent linkage at activated PEG on the liposomal surface or post-insertion of DSPE-PEG-antagonist G conjugates into pre-formed liposomes). The potential of the antagonist G-targeted formulations to associate with the target SCLC cells was studied by fluorescence microscopy using fluorescence-labelled liposomes and confirmed with radiolabelled [$^3$H]-CHE-liposomes. We also evaluated whether the presence of antagonist G at the membrane surface of the liposomes could significantly alter their biodistribution in healthy mice.

## 2. Materials and methods

### 2.1. Materials

The lipids 1,2-distearoyl-*sn*-glycero-3-phosphocholine (DSPC); cholesterol (CHOL); 1,2-dioleoyl-3-dimethylammonium-propane (DODAP); 1,2-distearoyl-*sn*-glycero-3-phosphoethanolamine-N-[methoxy(poly(ethylene glycol)-2000] (PEG-DSPE); 1,2-distearoyl-*sn*-glycero-3-phosphoethanolamine-N-[maleimide(polyethylene glycol)-2000] (Mal-PEG-DSPE); N-palmitoyl-sphingosine-1-(succinyl[methoxy(polyethylene glycol)2000]) (PEG-CerC16); L-α-phosphatidylethanolamine-N-(lissamine rhodamine B sulfonyl) (Rho-PE) were purchased from Avanti Polar Lipids (Alabaster, USA). Egg phosphatidylcholine (EPC) was acquired from Lipoid GmbH (Germany). 2-Iminothiolane·HCl (Traut's reagent) was purchased from Fluka (Buchs, Switzerland). Sephadex G-50 and Sepharose CL-4B were purchased from Pharmacia (Uppsala, Sweden), 4-(2-hydroxyethyl)-1-piperazineethanesulfonic acid (HEPES), 2-(N-Morpholino)-ethanesulfonic acid (MES), RPMI 1640; penicillin–streptomycin; fetal bovine serum (FBS), poly-L-lysine and Trypan Blue solution were purchased from Sigma Chemical Co. (St. Louis, MO, USA). TrypLE™ Express was purchased from Gibco (Grand Island, NY, EUA) and 4′,6-diamidino-2-phenylindole (DAPI) was provided by Instituto de Medicina Molecular (iMM) from Faculdade de Medicina da Universidade de Lisboa. The CHOD–POD enzymatic colorimetric assay for the determination of cholesterol was purchased from Spinreact (Sant Esteve de Bas, Spain). [1α,2α(n)–$^3$H]Cholesteryl hexadecyl ether, 1.48–2.22 TBq/mmol ([$^3$H]CHE) was purchased from Perkin-Elmer, Inc. (Waltham, USA). All other chemicals were of analytical grade.

The hexapeptide antagonist G (H-Arg-D-Trp-N$^{me}$Phe-D-Trp-Leu-Met-$NH_2$) was synthesized by Alberta Peptide Institute (Edmonton, AB, Canada) with a purity > 95%. The 16-mer phosphorothioate oligodeoxynucleotide was synthesized by TriLink BioTechnologies, Inc. (San Diego, USA), purity was > 95% by high-performance liquid chromatography analysis. The asODN referred to hereafter as *as(c-myc)* is complementary to the translation region of human *c-myc* mRNA and has the sequence 5′-TAACGTTGAGGGGCAT-3′.

### 2.2. Cell lines and mice

The human classical SCLC cell line NCI-H69 (ATCC HTB-119) and the human variant SCLC cell line NCI-H82 (ATCC HTB-175) were obtained from the American Type Culture Collection. Both cell lines were cultured in RPMI 1640 supplemented with 10% (v/v) heat–inactivated FBS, 100 U/mL penicillin, 100 μg/mL streptomycin, 1 mM sodium pyruvate, 1.5 g/L sodium bicarbonate, 2.5 g/L glucose and 25 mM HEPES for H69 or 10 mM HEPES for H82, pH 7.4 (full medium). Cell lines were

maintained in the logarithmic phase of growth at 37 °C in a humidified incubator (90% humidity) containing 5% $CO_2$.

BALB/c mice, 6 to 8 weeks old, were purchased from Gulbenkian Institute of Science (Oeiras, Portugal), and housed at Faculdade de Farmácia da Universidade de Lisboa animal facilities. The animals were kept under standard hygiene conditions, fed commercial chow and given acidified drinking water ad *libitum*. All animal experiments were carried out with the permission of the local animal ethics committee, and in accordance with the Declaration of Helsinki, EEC Directive (2010/63/UE) and Portuguese Law (DL 113/2013, Despacho n° 2880/2015), and all following legislation for the humane care of animals in research.

### 2.3. Preparation of liposomes

The lipid compositions of the non-targeted and targeted formulations used in this work are shown in Table 1.

#### 2.3.1. Long circulating liposomes (LCL)

The lipidic composition of this formulation consisted of EPC:CHOL:PEG-DSPE at 68.25:30.5:1.25 M ratio. The liposomes were prepared by lipid film hydration method, using 10 mM citrate buffer, 145 mM NaCl, pH 6.0 for hydration. The resulting multilamellar vesicles suspension was sequentially extruded through polycarbonate membranes (Nucleopore filters®) with a pore diameter ranging from 0.6 to 0.05 μm to yield a monodisperse liposomal suspension. The liposomal formulations were purified by ultracentrifugation at 300 000 × *g*, for 2 h at 15 °C, in an Optima™ XL-90 Ultracentrifuge (Beckman Coulter, USA) with a 70 Ti rotor.

The fluorescent LCL formulations were labelled with rhodamine B (0.25 % mol of total lipid) and prepared as described above. Before use liposomes were filtered through a PTFE filter with a pore diameter of 0.2 μm.

#### 2.3.2. Stabilized antisense lipid particles (SALP)

Preparation of SALP with or without the encapsulation of *as(c-myc)* was performed by the ethanol dilution method adapted from Semple *et al.* (Semple et al., 2001). Briefly, a lipid mixture of DSPC:CHOL:DODAP:PEG-Cer$C_{16}$ (20:45:25:10 mol%, 13 μmol total lipid) in absolute ethanol was heated at 65 °C and added drop by drop to 2 mg of the *as(c-myc)* in 300 mM citrate buffer, pH 4.0 (or 300 mM citrate buffer, pH 4.0 for empty SALP) at 65 °C under vigorous mixing. The suspension was extruded at 65 °C twice through 0.2 μm and 10 times through 0.1 μm polycarbonate membranes using a thermobarrel extruder (Lipex Biomembranes, Vancouver, Canada). The lipid vesicles were dialyzed (12–14 kDa cut-off) against 300 mM citrate buffer, pH 4.0 for 2 h to remove excess ethanol, leading to formation of multilamellar vesicles (Semple et al., 2001). DODAP was neutralized by the removal of the citrate buffer from the preparation through a further overnight dialysis against HBS buffer (20 mM HEPES, 145 mM NaCl, pH 7.6). The final SALP were obtained by ultracentrifugation (250 000 × *g* for 2 h) in a Beckman LM-80 M ultracentrifuge (Beckman Instruments, Inc., Fullerton, USA).

Radiolabelled SALP formulation was prepared incorporating the non-exchangeable tritium-labelled lipid cholesteryl hexadecyl ether ([$^3$H]CHE) (55.5 kBq/ μmol of total lipid). The lipid concentration was determined by the specific activity (cpm/μmol TL) from β–counts using a LS-6800 counter (Beckman Instruments, Fullerton, USA).

**Table 1**
Lipid composition of the different types of liposomal formulations evaluated in this study. The corresponding names are used throughout the text to identify the formulations.

| Formulation name | Lipid Composition | Molar ratio |
|---|---|---|
| **Non-targeted** | | |
| LCL | EPC:CHOL:DSPE-PEG | 68.25:30.5:1.25 |
| SALP | DSPC:CHOL:DODAP:Cer$C_{16}$-PEG | 20:45:25:10 |
| **Antagonist G-targeted** | | |
| **Direct method** | | |
| G-LCL | EPC:CHOL:DSPE-PEG:DSPE-PEG-Mal | 68.25:30.5:0.55:0.7 |
| G-SALP | DSPC:CHOL:DODAP:Cer$C_{16}$-PEG: DSPE-PEG-Mal | 20:45:25:8:2 |
| **Post-insertion method** | | |
| PI(G-LCL) | EPC:CHOL:DSPE-PEG:DSPE-PEG-Mal | 68.25:30.5:0.55:0.7 |
| PI(G-SALP) | DSPC:CHOL:DODAP:Cer$C_{16}$-PEG: DSPE-PEG-Mal | 20:45:25:8:2 |

LCL – Long Circulating Liposomes; SALP – Stabilized Antisense Lipid Particles containing ionizable amino lipid; G-LCL – Antagonist G-targeted LCL (direct method); G-SALP – Antagonist G-targeted SALP (direct method); PI(G-LCL) – Antagonist G-targeted LCL (post-insertion); PI(G-SALP) – Antagonist G-targeted SALP (post-insertion).

#### 2.3.3. Antagonist G-targeted liposomes

Two methods were used for the coupling of antagonist G (H-Arg-DTrp-N-$^{me}$Phe-DTrp-Leu-Met-$NH_2$) to the formulations. In both methods the antagonist G was covalently linked to PEG-derivatized DSPE using a maleimide – thiol reaction (Kirpotin et al., 1997). Regardless the coupling procedure, an appropriate volume of a 5 mM solution of antagonist G in water was thiolated at the N-terminus by 2-iminothiolane (20 mM), at an iminothiolane:antagonist G molar ratio of 4:1, for reactivity toward the maleimide. Silicon-coated glassware (Sigmacote, Sigma) was used for this reaction which occurred in HEPES buffer, pH 8.0, for 1 h at room temperature.

*2.3.3.1. Direct coupling method.* The thiolated antagonist G was added to pre-formed LCL and SALP at an antagonist G:lipid molar ratio of 1:100 the vial sealed under $N_2$ stream. The reaction took place for 12 to 18 h at room temperature. For the G-SALP formulation, potential free maleimide groups were quenched with 2–mercaptoethanol in HEPES buffer, pH 6.5, at room temperature for 30 min. The targeted formulations were separated from non-coupled antagonist G by ultracentrifugation (180 000 × *g*, 2 h for G-SALP and 300 000 × *g*, 2 h for G-LCL). The G-SALP and G–LCL pellets were suspended in HEPES buffer, pH 7.4 or 10 mM citrate buffer, 145 mM NaCl, pH 6.0, respectively.

*2.3.3.2. Post-Insertion method.* Mal-PEG-DSPE micelles were prepared at a concentration of 0.5 mM in HEPES/MES buffer (25 mM HEPES, 25 mM MES, 140 mM NaCl, pH 6.5 and added to the thiolated antagonist G at a 2:1 Mal-PEG-DSPE:antagonist G molar ratio for SALP and at a 1:1.4 (Mal-PEG-DSPE:antagonist G) for LCL. The coupling reaction was performed overnight at room temperature, in an inert $N_2$ atmosphere. Free maleimide groups were neutralized as described above for the direct coupling method.

Antagonist G-coupled PEG-DSPE micelles were incubated 1 h with non-targeted SALP at 60 °C and with non-targeted LCL at room temperature to promote the insertion of antagonist G-PEG-DSPE conjugates into the lipid bilayer. The resulting targeted PI(G-SALP) were purified by gel filtration through a Sepharose CL–4B column (Pharmacia, Sweden) equilibrated with HEPES buffer, pH 7.4 and PI(G-LCL) were purified by ultracentrifugation as described for the direct method and suspended in 10 mM citrate buffer, 145 mM NaCl, pH 6.0.

Radiolabelled G-SALP formulation was prepared as described in the section 'Stabilized Antisense Lipid Particles (SALP)'.

### 2.4. Physicochemical characterization of the liposomal formulations

The mean particle diameter determined as Z-average (Ø) and the polydispersity index (PdI) were assessed by quasi-elastic laser light scattering in a Malvern Zetasizer Nano S (Malvern Instruments, UK). The zeta potential (surface charge, ξ) was determined using laser Doppler velocimetry in a Nano Z (Malvern Instruments, UK). Samples were appropriately diluted with buffer for the measurements and the same

voltage was applied to each measurement.

Lipid content of the final formulations was determined by different methods due to specific interferences of other formulation components.

For formulations containing as(c-myc), lipid content was inferred from cholesterol concentration using an enzymatic-colorimetric (CHOD-POD) based commercial kit (Spinreact, Spain). The total phospholipid content of empty formulations was determined by the Rouser method, as previously described (Rouser et al., 1970). Whenever formulations were labelled with the non-metabolizable, non-exchangeable radioactive tracer, [$^3$H]CHE, the total lipid concentration was determined from the specific activity counts of the [$^3$H]CHE tracer in a Beckman LS-6800 Scintillation counter (Beckman Instruments, Fullerton, USA).

Determination of the amount of antagonist G coupled to the liposomes was based on the quantification of the tryptophan residue present in the peptide by fluorimetry using $\lambda_{ex} = 288$ nm and $\lambda_{em} = 330$ nm in a Hitachi F-3000 Fluorescence Spectrophotometer (Hitachi High-Technologies Corporation, Tokyo, Japan).

The amount of *as(c-myc)* was determined by spectrophotometry at 260 nm in a Shimadzu UV-160A spectrophotometer (Shimadzu Corporation, Kyoto, Japan). Before quantification, liposomes were disrupted to release all the encapsulated *as(c-myc)*. The concentration was calculated according to Eq. (1), where 30.7 μg/mL corresponds to the extinction coefficients for phosphorothioate oligodeoxynucleotides.

$$[as(c-myc)](\mu g/mL) = A_{260} \times 30.7 \mu g/mL x 1.1 mL/\text{sample volume}(\mu L) \quad (1)$$

The encapsulation parameters used to characterize all the formulations were Encapsulation Efficiency (E.E.) and the Insertion Capacity (I.C.) (when applied). The Encapsulation Efficiency (E.E.) was expressed as the percentage of the ratio between the final and the initial *as(c-myc)* to lipid ratio and was calculated from Eq. (2).

$$[(as(c-myc)/\text{Lip})\text{finalratio}/(as(c-myc)/\text{Lip})\text{initialratio}] \times 100 \quad (2)$$

The Insertion Capacity (I.C.), defined as the amount (in grams) of antagonist G, per mol of lipid determined after preparation, was used to characterize the antagonist G–targeted formulations.

### 2.5. Cellular association studies

These studies were performed quantitatively with rhodamine B fluorescent or [$^3$H]-CHE radiolabelled liposomes.

#### 2.5.1. Assessment by fluorescence microscopy

H69 cells were disaggregated by passing through a 5 mL pipet and were plated at $1 \times 10^5$ cells/well in 24-well plates. The liposomal formulation was added at a concentration of 0.25 mM in RPMI medium. Incubation took place at 37 °C, for 1 h and 3 h, in a humidified atmosphere containing 5% $CO_2$.

After the incubation, cells were centrifuged at 134 × *g* for 5 min in an Eppendorf® Microcentrifuge 5415D (Hamburg, Germany) and were washed 3 times with PBS at 4 °C. After the third centrifugation, the pellet was suspended in the residual volume of the tube and cells were processed for immunofluorescence microscopy.

For observation of live cells, a drop of the cellular suspension was placed on a microscope slide, covered with a cover slip and immediately observed under the microscope. For fixed cells, the cell suspension was added on top of poly-L-lysine Sigma (St. Louis, USA) pre-coated coverslips, and let to adhere. The coverslips were washed with ice-cold PBS, fixed with 3.7% (m/v) paraformaldehyde, stained with DAPI (1 μg/mL), rinsed with ice-cold PBS and embedded in the Mowiol mounting media. In both cases immunofluorescence microscopy was performed using the Olympus BX41 microscope (PlanApo objective, 60x magnification), equipped with an Olympus U-RFL-T lamp (Japan). The images were taken with an Olympus CAMEDIA C-4040 ZOOM digital camera using the Cam2Com 4.1 – Digital Camera Control Software, Sabsic. Images were processed with ImageJ Fiji software (NIH, USA) and the Adobe Photoshop software (Adobe Systems, San Jose, CA).

#### 2.5.2. Binding, uptake, competition, and endocytosis inhibition in vitro studies

These studies were performed with both the H69 and H82 SCLC cell lines. The cells were plated at $1 \times 10^6$ cells/well (100 μL) in 48-well plates and incubated at 37 or 4 °C, during 1 h, with [$^3$H]CHE-SALP and [$^3$H]CHE-PI(G-SALP) at concentrations ranging from 0.1 to 0.8 mM of total lipid. For the competition experiments, H82 cells were pre-incubated with either non-radiolabelled liposomes (Lip) or antagonist G-coupled liposomes (G-Lip) at 0.6 μg antagonist G/well for 30 min at 37 °C before the addition of [$^3$H]CHE-PI(G-SALP) and incubated in the same conditions for 1 h. For the experiments with endocytosis inhibitors, H82 cells were pre-incubated for 30 min at 37 °C with 0.45 M sucrose/well. After the pre-incubation period [$^3$H]CHE-PI(G-SALP) were added and the incubation proceeded at 37 °C in a humidified atmosphere containing 5% $CO_2$ in air for 1 h. After incubation, 750 μL of PBS buffer at 4 °C, pH 7.4 (137 mM NaCl, 2.68 mM KCl, 8.10 mM $Na_2HPO_4$, 1.47 mM $KH_2PO_4$) was added to each well and the plates were centrifuged at 220 × g for 10–12 min. The supernatant was aspirated, and an additional 1 mL of the same buffer was added. This procedure was repeated once more, for a total of three washes, and the cells were resuspended in 0.5 mL PBS, pH 7.4. The cellular suspension of each well was then transferred to scintillation vials with 5 mL of aqueous counting scintillant (ACS). Cellular association of liposomes was calculated from the specific activity of the lipid label [$^3$H]CHE in liposomes and was expressed as nmol of total lipid (TL)/$10^6$ cells.

### 2.6. Tissue distribution studies

Male BALB/c mice, (20–25 g) received injections via tail vein (i.v.) of a single dose of SALP liposomes (targeted or non-targeted), in a total volume of 0.2 mL (1 μmol Lip/mouse). At selected time points (30 min, 2 h, 6 h and 24 h post-injection) groups of four mice per liposomal formulation were anesthetized and sacrificed by cervical dislocation. A blood sample was withdrawn from the retro orbital sinus before sacrifice, and the liver, spleen and lungs were excised. The blood (50 μL) and organ (50 μg) samples were discoloured with 0.2 mL of hydrogen peroxide and 0.1 mL of perchloric acid overnight in an oven at 50 °C. Samples were then neutralized with 0.1 mL of acetic acid and transferred to 10 mL Hionic Fluor scintillation fluid. Total radioactivity was measured using a Beckman LS–6800 Scintillation beta counter (Beckman Instruments, Fullerton, USA). Aliquots of the injected liposomes (10 μL) before and after being subjected to the same treatment as the samples were simultaneously counted to correct the physical decay. The results were expressed as percentage of the injected dose per mL of blood or gram of tissue.

### 2.7. Statistical analysis

The statistical analysis was performed with one-way analysis of variance (ANOVA) followed by Tukey's multiple comparison test using the software Graph Pad Prism version 7.0 (CA, USA. Significance levels obtained are described in figure legends.

## 3. Results

Antagonist G-targeted liposomal formulations for the selective delivery of anticancer drugs to SCLC cells were prepared based either on previously described PEG long circulating liposomes (LCL) (Marcelino et al., 2017) or on stabilized lipid particles (SALP) (Semple et al., 2001). Two different methods were used to covalently link Antagonist G to the liposomal surface: post insertion and direct coupling. We started by evaluating how the phospholipid composition of the liposome bilayer, preparation method and coupling method used for the liposomal

formulations affected their targeting efficiency to SCLC cell lines *in vitro*.

### 3.1. The amount of antagonist G present at the liposomal surface is affected by the phospholipid composition of the bilayer and by the preparation method

Our studies focused first on the characterization of the antagonist G-targeted formulations prepared by different methodologies, including the phase transition temperature of the major phospholipid (EPC vs DSPC), the pH of the buffer used and the physical properties of the final liposomes (Table 2). The effect of the presence of antagonist G at the liposomal surface on the properties of the LCL and SALP formulations was also evaluated. The mean size and homogeneity of the liposome population were similar in the various formulations meaning that the coupling of antagonist G did not change the average size of the liposomes. These results were expected since antagonist G is a small peptide (only six amino acid residues). Moreover, since antagonist G has no net charge, the zeta potential did not change either, as confirmed by the values obtained.

The amount of antagonist G present at the liposomal surface was affected by the lipid composition of the bilayer and by the preparation method (Table 2). In order to evaluate the effect that the levels of antagonist G display in liposomes ability to associate with cells, all the formulations – with the exception G–SALP – were used for the *in vitro* studies. Liposomal formulations containing 0.25 mol% rhodamine B (Rho-PE) were prepared to perform *in vitro* cellular association studies using fluorescence microscopy. The inclusion of Rho-PE in the liposomal formulations did not change their characteristics (data not shown). The fluorescence intensity of the Rho-PE labelled formulations was measured to warrant an accurate comparative analysis of the extent of cellular association between the different formulations. As can be observed in Table 2, similar fluorescence emission levels were obtained for formulations with the same lipidic concentration irrespective of the preparation method. For formulations with different compositions (LCL vs SALP and PI(G-LCL) vs PI(G-SALP), Table 1) the results were further apart probably because of the different preparation methods used.

### 3.2. The presence of antagonist G on the liposome surface enhances cellular association into SCLC cells but lipid bilayer composition has no effect on the internalization of the formulations

Cellular association experiments using fluorescence microscopy and Rho-PE labelled liposomes were carried out to determine whether the different lipid composition of the liposomal bilayer (LCL and SALP) and the coupling methods (direct and post-insertion) would affect the ability of antagonist G to target the human SCLC cell line H69 *in vitro* (Fig. 1 and Fig. 3).

To demonstrate that all the fluorescence observed was due to the Rho-PE liposomes either bound or internalized by the cells, non-labelled liposomes and cells alone were used as negative controls.

Rhodamine B fluorescence intensity depicted in Fig. 1 was quantitatively evaluated through the normalization of each sample to H69 cells where no formulation was added (Fig. 2).

Cellular background autofluorescence in the rhodamine B filter was vestigial, being statistically different ($P < 0.001$) in comparison to cells that were incubated with a formulation and, as for liposomes, they were eliminated in the washing process (Fig. 1 panel A, and B and Fig. 2). Therefore, we can assume that the observed fluorescence was only related to the binding of Rho-PE liposomes and their possible internalization, which is supported by the images in Fig. 1. As can be observed in Fig. 1(C), the red fluorescence intensity imparted by the fluorophore was similar for the two non-targeted formulations (LCL and SALP) at both incubation times. This result was confirmed by the quantitative analysis, where no significant differences were found for these formulations (Fig. 2). For antagonist G-targeted liposomes (G-LCL, PI(G-LCL), PI(G-SALP)) the fluorescence intensity of rhodamine B was significantly higher when compared to non-targeted liposomes for a longer incubation period (3 h) indicating a higher extent of binding and internalization of antagonist G-targeted liposomes by the cells. This result is in agreement with the increase in cellular association (composed of the binding of the liposomes to the cell surface and subsequent internalization) previously observed by Moreira et al. for antagonist G-targeted liposomes during more than 4 h (Moreira et al., 2001). The increase of fluorescence intensity with the incubation time may be due to an increased rate of receptor-mediated endocytosis for receptors recognized by antagonist G and indicates that antagonist G receptors were not saturated by the antagonist G-targeted formulations herein used. In fact, an increased rate of receptor-mediated endocytosis is to be expected up until the receptors are saturated. From that point on, mediated endocytosis reaches a steady-state due to the recycling of receptors which after being transported to the cell surface will again be able to recognize and bind more ligands and internalize them. It should be noted that the distribution of the antagonist G-targeted formulations in the cells was not homogeneous. This may be related either to cellular variability in the expression of receptors that recognize this targeting agent or, since cells grow in aggregates, to a more difficult access of targeted liposomes to core cells. In order to minimize the effects of the latter factor, cell aggregates were disrupted before the experiment was started. However, we did not obtain individualized cells and so, cell aggregation could be interfering with the results obtained.

To confirm the previous results obtained with live cell imaging and to determine more accurately the intracellular location of liposomes, additional cellular association studies were performed where H69 cells were fixed and analysed by fluorescence microscopy. As observed in Fig. 3 (panel A and B) and Fig. 4, the autofluorescence of H69 fixed cells detected with the rhodamine B filter was not meaningful and both LCL and SALP non-targeted formulations were totally eliminated in the washing process. Therefore, the red fluorescence visible in Fig. 2(C) was due to the labelled liposomes that may have been internalized by the cells. However, it was not possible to determine the intracellular location of the liposomes since H69 cells have a small cytoplasm.

As observed in live-cell imaging, both LCL and SALP non-targeted

**Table 2**
Physico-chemical characterization of antagonist G-targeted and non-targeted liposomes.

| Formulation | Hydrodynamic diameter (μm) | Zeta potential (mV) (pH 6.0) | [Lip]f (mM) | [Ant G/Lip]f (g /mol) | [a]Rho-PE Fluorescence Intensity (u.a.) |
|---|---|---|---|---|---|
| **LCL** | 0.11 ± 0.01 | −1.99 ± 0.54 | 15.3 ± 1.1 | n.a. | 5594 ± 31 |
| **G-LCL** | 0.11 ± 0.01 | −2.24 ± 0.32 | 15.5 ± 1.3 | 5.1 ± 1.1 | 5116 ± 190 |
| **PI(G-LCL)** | 0.12 ± 0.01 | −2.32 ± 0.48 | 13.9 ± 1.7 | 2.6 ± 0.1 | 5238 ± 571 |
| **SALP** | 0.09 ± 0.01 | −1.41 ± 0.41 | 10.0 ± 0.5 | n.a. | 4372 ± 33 |
| **G-SALP** | 0.10 ± 0.01 | −2.15 ± 0.81 | 6.0 ± 0.5 | 5.6 ± 0.8 | n.d. |
| **PI(G-SALP)** | 0.10 ± 0.01 | −1.86 ± 0.41 | 6.1 ± 1.0 | 8.2 ± 0.6 | 3881 ± 219 |

The indicated values are the median ± standard deviation obtained in $n \geq 3$ independent experiments. Targeted formulations were coupled at a 1:100 antagonist G/Lipid molar ratio. n.a. – not applicable. All formulations had a polydispersity index below 0.2. Lip - total lipid; Ant G – Antagonist G.

[a] Fluorescent intensity of Rho-PE-labelled liposomes (10 mM total lipid). The indicated values are average ± standard deviation obtained in $n = 2$ independent experiments.

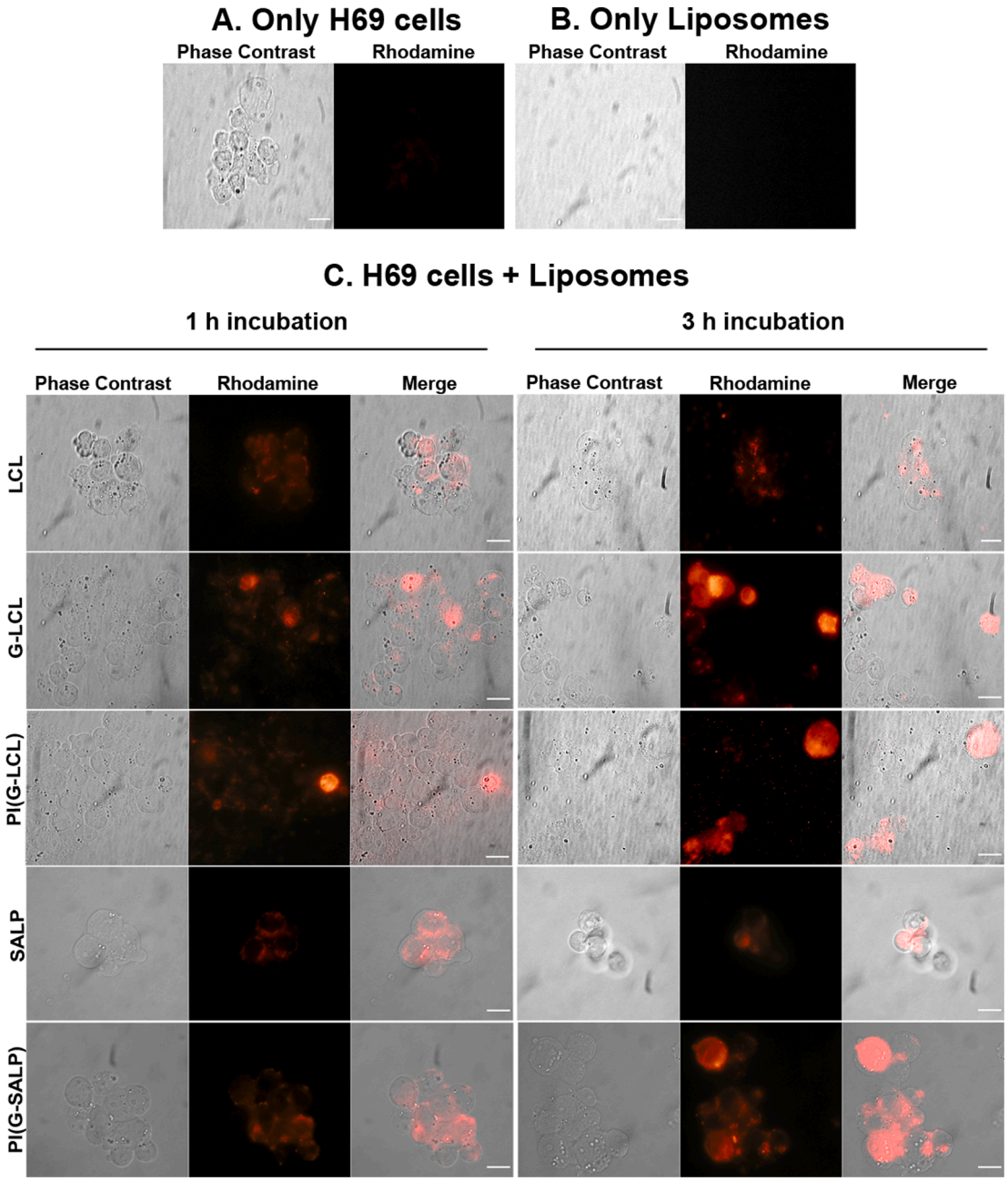


**Fig. 1. Cellular association of Antagonist G-targeted and non-targeted liposomes with H69 live cells analysed by fluorescent microscopy.** Representative images of phase-contrast and fluorescent microscopy of (A) control for H69 cells autofluorescence, (B) negative control for non-labelled liposomes and (C) non-fixed H69 cells incubated at 37 °C with Rho-PE-labelled (red) liposomes at 0.25 mM of total lipid, after 1 h (left panel) and 3 h (right panel) of incubation. The images were obtained with phase contrast (left) or filters for rhodamine B (middle). The merged images were obtained with the software ImageJ Fiji (NIH, USA). These results are from one representative experiment (n = 3). White bar – 10 μm.

formulations displayed similar levels of fluorescence (non-significant difference between LCL and SALP), but lower than the antagonist G-targeted formulations (Fig. 3 (C) and Fig. 4). Also, for non-targeted liposomes, a longer incubation time of the liposomal preparations with cells (3 h), led to a red fluorescence level in cells similar to that at 1 h incubation. This may have been due to a saturation of non-specific binding and endocytosis of non-targeted liposomes in H69 cells. On the contrary, when antagonist G-targeted liposomal formulations were added to cells, the red fluorescence levels conferred by rhodamine B was statistically different even after 1 h incubation as indicated in Fig. 4, and it increased over time, which, as in the case of non-fixed cells, agrees with results obtained in other studies (Moreira et al., 2001). Rhodamine B labelling of cells after 3 h of incubation with antagonist G-targeted liposomes indicates an increased liposomal binding to cells and, possibly, a greater internalization of PI(G-LCL), followed by PI(G-SALP) and, finally, G-LCL liposomal formulations. This ranking for the increase in red fluorescence of cells inversely correlates with the levels of antagonist G at the surface of each of these liposomal preparations (Table 1), except for PI(G-SALP) whose red fluorescence was lower than G-LCL. Despite PI(G-SALP) being the formulation with the highest level of antagonist G, it displayed the lowest intensity of rhodamine B fluorescence (Table 1) which could be causing the inversion of the fluorescence order of these two formulations. Therefore, it is possible that the amount of antagonist G at the surface of liposomes with neutral lipids does not cause saturation of antagonist G receptors on the surface of H69 cells, otherwise more similar fluorescence levels would be expected

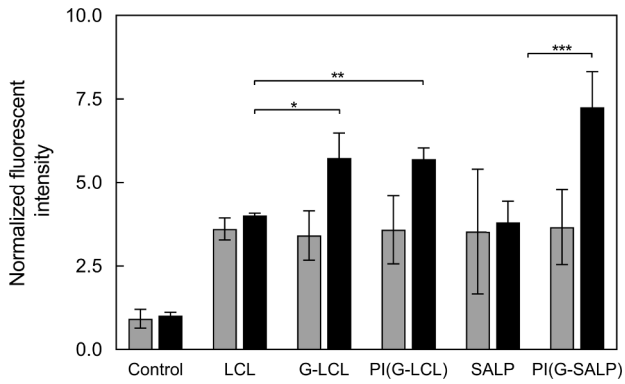


**Fig. 2. Quantification of cellular association of Antagonist G-targeted and non-targeted liposomes with H69 live cells analysed by fluorescent microscopy.** Quantification of rhodamine B fluorescence of non-fixed H69 cells incubated for 1 h (grey bars) or 3 h (black bars) at 37 °C with Rho-PE-labelled liposomes at 0.25 mM of total lipid. Data are presented as the mean ± standard deviation of the fluorescence intensity of each condition normalized to the autofluorescence obtained for H69 cells (control) from 3 independent experiments with a minimum of 20 cells analysed per condition. * $P < 0.05$, ** $P < 0.01$, *** $P < 0.001$ ($n = 3$).

between all antagonist G-targeted liposomes studied.

In conclusion, while lipid composition had no effect on the internalization of formulations by SCLC cells, the incorporation of antagonist G on the liposomal surface and its retention in liposomes was dependent on the composition of the lipid bilayer. As such, G-LCL liposomal formulations should be selected for incorporation of low molecular weight molecules, due to achievement of high liposomal binding and internalization, and G-SALP for negatively charged genetic material, due to the charges interaction that enable a higher loading capacity.

### *3.3. Application of SALP formulations for intracellular delivery of an antisense oligonucleotide as(c-myc) to SCLC cells in vitro and in vivo*

An antagonist G-targeted formulation incorporating the asODN (as (c-*myc*)) was prepared and evaluated *in vitro* regarding its ability to be delivered intracellularly into SCLC cell lines and *in vivo* to see whether it accumulated in the target organ (lungs).

#### *3.3.1. as(c-myc) can be efficiently encapsulated in SALP liposomes*

To mediate the intracellular delivery of *as(c-myc)* to SCLC cells we selected the SALP formulation containing the ionizable amino lipid DODAP. Antagonist G was attached to the SALP surface to promote specific targeting to tumour cells leading to efficient intracellular delivery as anticipated by the cellular association results of the empty formulation (Figs. 1 and 3). The SALP formulations containing *as(c-myc)* were developed to have a mean size around 100 nm and a polydispersity index below 0.20. These characteristics are critical for systemic delivery and efficient tumour accumulation of liposomes containing anti-cancer drugs (Moura et al., 2012). The encapsulation parameters and physico-chemical characterization of antagonist G-targeted and non-targeted SALP displayed in Table 3 showed that, irrespective of the presence of Antagonist G, all formulations exhibited suitable particle sizes and a membrane charge representative of a neutral formulation (zeta potential of $-5 \pm 1$ mV) due to the presence of the PEG coating.

The covalent linkage of antagonist G to the SALP surface by the two proposed methods caused a reduction of the *as(c-myc)* loading capacity. This was probably due to the incubation step necessary for antagonist G coupling. When comparing both antagonist G-targeted liposomal formulations, the one using the post-insertion method displayed a higher E. E.. This result suggests that the insertion of antagonist G conjugates to the surface of preformed SALP is a valid method to prepare the antagonist G-targeted formulation for the remaining studies.

#### *3.3.2. The presence of antagonist G at the surface of SALP containing as-(c-myc) increases their association with SCLC cells*

As previously demonstrated (Fig. 2 and Fig. 4), the presence of antagonist G at the surface of different liposomal formulations increased their association to SCLC cells *in vitro*. Antagonist G specific targeting and the extent of cellular association and internalization of PI(G- SALP) prepared by the post insertion method and containing *as(c-myc)*, was further evaluated both in a classical (H69) and a variant (H82) human SCLC cell line, and compared to non–targeted SALP of similar composition (Fig. 5). The H82 cell line grows in floating cellular aggregates as the H69 cell line (Moreira and Gaspar, 2004; Moreira et al., 2001), but is a more aggressive type of SCLC with increased cell proliferation and less responsive to chemotherapy than H69 cells. All formulations were labelled with [$^3$H]-CHE and incubated with SCLC cells at various concentrations and at two different temperatures (4 °C and 37 °C) as previously described in the methods section.

The higher extent of cellular association observed in Fig. 5 for G-SALP when compared to the corresponding non–targeted formulation demonstrated the ability of the coupled antagonist G to improve the cellular association to the SCLC cell lines, in a lipid dose-dependent manner. The higher cellular association levels obtained for G-SALP in the experiments carried out at 37 °C when compared to those achieved at 4 °C (a temperature that is non–permissive for endocytosis), strongly suggested that antagonist G-targeted liposomes were being actively internalized by SCLC cells.

The cellular association profile for G-SALP showed a maximum of 18.8 and 19.1 nmol lipid/$10^6$ cells for H69 and H82 respectively, at a lipid concentration of 1.6 mM. At this concentration, the uptake of G-SALP was about 17-fold higher than for non-targeted SALP, for both cell lines (Fig. 5(A) and (B)). This increased uptake reinforces the hypothesis that the liposomal internalization was mediated by antagonist G receptors. At 4 °C, an average 2.1–fold decrease in the cellular association of G-SALP was observed in both cell lines. This difference indicates that part of the cell–liposome association observed at 37 °C corresponds to liposome internalization by the tumour cells.

#### *3.3.3. Antagonist G-targeted liposomes are internalized by receptor–mediated endocytosis*

Another set of experiments was performed to confirm that G-SALP internalization was receptor-mediated and to elucidate the mechanism of internalization. In these assays H82 cells were pre-treated either with non-radiolabelled antagonist G-coupled to long circulating liposomes (G-LCL) and the corresponding non-targeted formulation (LCL) to perform competition studies or with 0.45 M sucrose, known to selectively inhibit clathrin–mediated endocytosis by blocking clathrin-coated pit formation (Heuser and Anderson, 1989). In all these experiments H82 cells were incubated with the various compounds and formulations 30 min before the addition of [$^3$H]–(G–SALP) (Fig. 6).

A decrease of 47% in the cellular association level of G-SALP was observed in Fig. 6 when H82 cells were treated with sucrose, as compared to the absence of endocytosis inhibitor. This result suggests that liposomes were internalized by receptor–mediated endocytosis.

In competition experiments non-targeted LCL did not interfere with the association of G-SALP to SCLC cells. This result was expected as LCL are neutral liposomes without a targeting agent. On the contrary, the association of G-SALP with H82 cells was competitively inhibited when cells were pre-incubated with non-radiolabelled G-LCL. This formulation was responsible for a 43% inhibition of the association of G-SALP with H82 cells. This inhibition was a clear indication that internalization of antagonist G-targeted liposomes is receptor-mediated.

In a different set of competition experiments, pre-incubation with free antagonist G (5 μg/well) did not competitively inhibit the binding of 0.4 mM of [3H]-CHE-(G-SALP). In this assay a non-targeted LCL formulation was used as control. The results obtained were $5.0 \pm 0.6$ and $4.2 \pm 0.3$ total lipid / $10^6$ H82 cells for pre-incubation with LCL formulation and free antagonist G, respectively. Similar results have

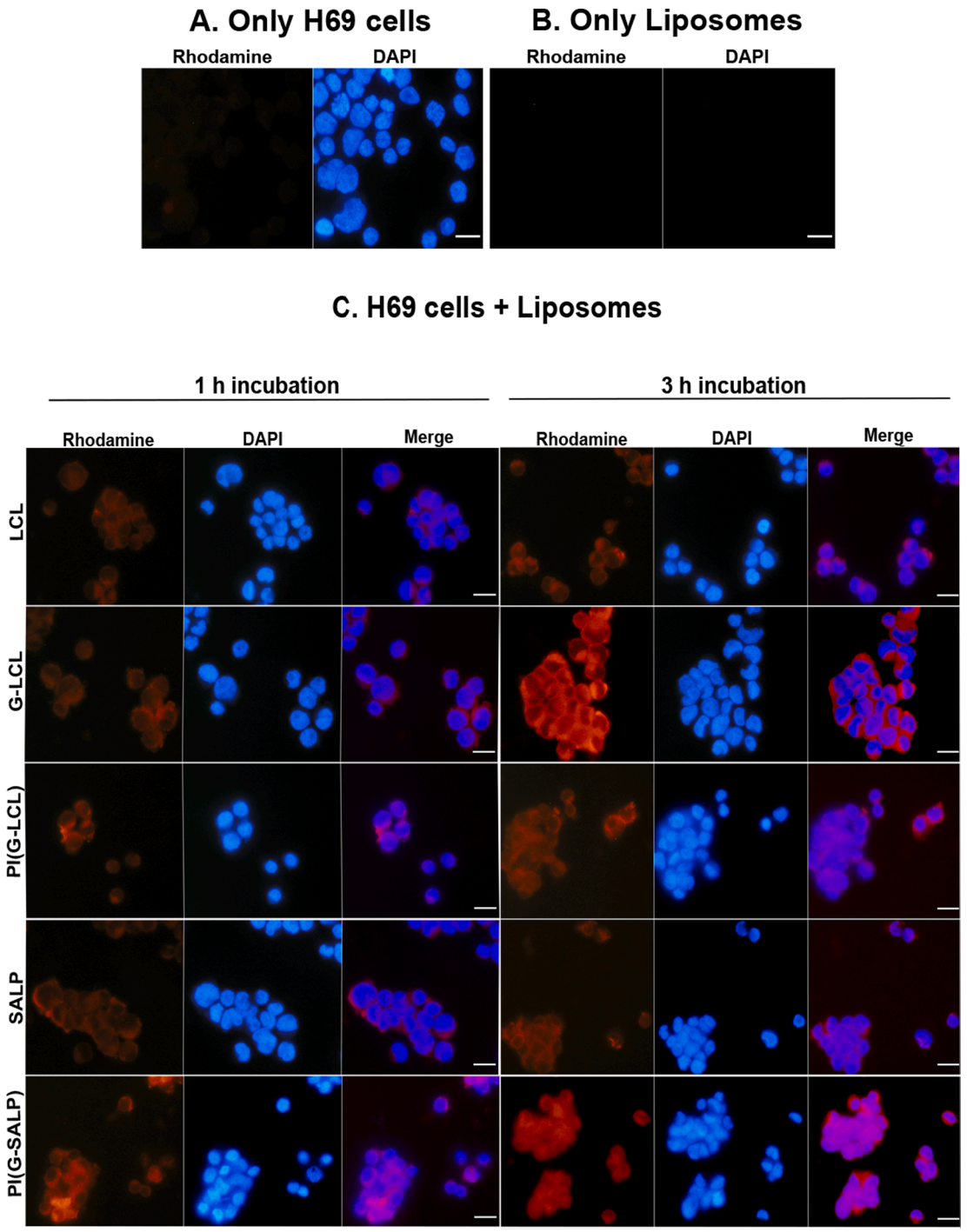


**Fig. 3. Cellular association of Antagonist G-targeted and non-targeted liposomes with fixed H69 cells analysed by fluorescent microscopy.** Representative images of fluorescent microscopy of (A) control for H69 cells autofluorescence, (B) negative control for liposomes and (C) H69 cells incubated at 37 °C with Rho-PE-labelled (red) liposomes at 0.25 mM total lipid after 1 h (left panel) and 3 h (right panel) of incubation, fixed after the incubation period. H69 cell nucleus was stained with DAPI (Peterman et al., 1993). The images were obtained with filters for DAPI (left) or rhodamine B (middle). The merged images were obtained with the software ImageJ Fiji (NIH, USA). These results are from one representative experiment (n = 3). Scale bar for all panels = 10 μm.

been obtained by other authors (14).

*3.3.4. as(c-myc)-containing antagonist G-targeted SALP liposomes have a higher accumulation in lungs and spleen*

We studied the blood profile of PI(G-SALP) and the biodistribution of PI(G-SALP) and non–targeted SALP containing *as(c-myc)* in order to see if these loaded liposomes accumulated in the lungs. The main characteristics of the liposomes used in these experiments are depicted in Table 4. The experiments were carried out in BALB/c mice with [$^3$H]-CHE-labelled formulations administered as a single bolus dose of 1.5 μmol of lipid.

The blood profile of PI(G-SALP) after i.v. injection into mice was determined (Fig. 7). After the first 6 h post injection about 40% of the injected dose is still present. After this time point, the rate of disappearance from the blood decreased but at a slower rate. At 24 h post-injection, around 12% of the injected dose was still present in the blood. These results demonstrate that the presence of the antagonist G at the surface of SALP does not affect the long-circulation characteristics of

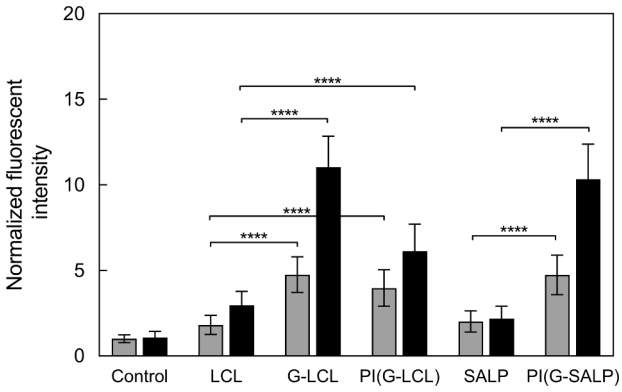


**Fig. 4. Quantification of cellular association of Antagonist G-targeted and non-targeted liposomes with H69 fixed cells analysed by fluorescent microscopy.** Quantification of rhodamine B fluorescence of H69 cells that were fixed after their incubation for 1 h (grey bars) or 3 h (black bars) at 37 °C with Rho-PE-labelled liposomes at 0.25 mM of total lipid. Data are presented as the mean ± standard deviation of the fluorescence intensity of each condition normalized to the autofluorescence obtained for H69 cells (control) from 3 independent experiments with a minimum of 26 cells analysed per condition. **** $P < 0.0001$.

**Table 3**
Physico-chemical characterization of Antagonist G-targeted and non-targeted SALP containing *as(c-myc)*.

| Formulation | Particle Size (μm) | *as(c-myc)*/Lipid ratio (g/mol) | E.E. (%) | Antagonist G/ lipid (g/mol) |
|---|---|---|---|---|
| SALP | 0.10 ± 0.01 | 125 ± 34 | 71 ± 22 | n.a. |
| G-SALP | 0.09 ± 0.01 | 48 ± 6 | 31 ± 4 | 2.4 ± 1.0 |
| PI(G-SALP) | 0.11 ± 0.01 | 58 ± 8 | 53 ± 5 | 1.7 ± 0.5 |

All formulations have PdI < 0.2. Zeta potential at pH 7.4 was −5 ± 1 mV. Targeted formulations were coupled at a 1:100 antagonist G/lipid ratio. Data are presented as mean ± standard deviation in n ≥ 3 independent experiments. n.a. – not applicable; E.E. – encapsulation efficiency.

the SALP liposomes, as expected due to the presence of PEG at the surface.

The tissue distribution of SALP and PI(G-SALP) formulations in the liver, spleen and lungs at different times is shown in Fig. 8. The pattern of biodistribution of these formulations in the examined tissues showed a preferential accumulation of SALP liposomes in the liver whereas the PI(G-SALP) formulation presents a tendency to accumulate in the spleen. In fact, the amount of PI(G–SALP) accumulated in the spleen, 24 h post-injection was 2.5-fold higher than that of SALP. As for the lung, our organ of interest, a preferential accumulation of PI(G–SALP) as compared to SALP was observed for all time points and at 24 h, a 3-fold higher accumulation was still observed, demonstrating the potential of antagonist G-target formulation as a therapeutic agent *in vivo*, for the treatment of small cell lung cancer.

## 4. Discussion

Several studies have established that the covalent attachment of appropriate targeting ligands to the surface of liposomes significantly

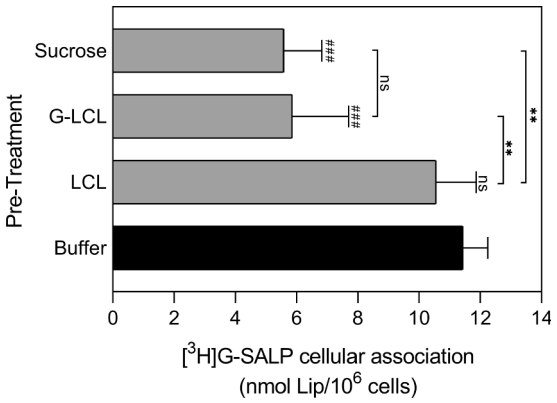


**Fig. 6. Effect of pre-treatment with sucrose, an endocytosis inhibitor, and competitive inhibition on the cellular association of [$^3$H] CHE-labelled G-SALP liposomes with H82 cells.** H82 cells (1x10$^6$ cells) were pre-incubated at 37 °C for 30 min with either the endocytosis inhibitor sucrose (0.45 M/well) or with 0.56 μg of antagonist G coupled to non-radiolabelled LCL (G-LCL) and non-targeted LCL (5 mM/well) for competitive inhibition studies. Buffer, which was used as control, was PBS pH 7.4. Inhibition was determined by adding [$^3$H] CHE-(G-SALP) (0.8 mM Lipid/well), at 37 °C for 1 h. Cellular association of liposomes was expressed as nmol of Lipid/10$^6$ cells. Each point is the mean ± standard deviation of three samples from one representative experiment. Statistical differences are denoted as $^{###}P < 0.001$ vs. buffer, and as $^{**}P < 0.01$ between indicated conditions ns - statistically non-significant.

**Table 4**
Characteristics of the [$^3$H]-CHE-labelled PI(G-SALP) and SALP liposomes.

| Formulation | Particle Size (μm) | L.C. (g/mol) | E.E. (%) | Antagonist G/lipid (g/mol) |
|---|---|---|---|---|
| PI(G-SALP) | 0.13 ± 0.01 | 45 ± 8 | 60 ± 9 | 7 ± 2 |
| SALP | 0.14 ± 0.01 | 55 ± 7 | 71 ± 5 | n.a. |

Targeted and non-targeted SALP liposomes composed of DSPC:CHOL:DODAP:PEG-Cer$C_{16}$:Mal-PEG-DSPE at 20:45:25:8:2 M ratio were prepared with 1 mg of *as(c-myc)* per 13 μmol (10 mg) of total lipid. E.E – encapsulation efficiency; L.C. - loading capacity.

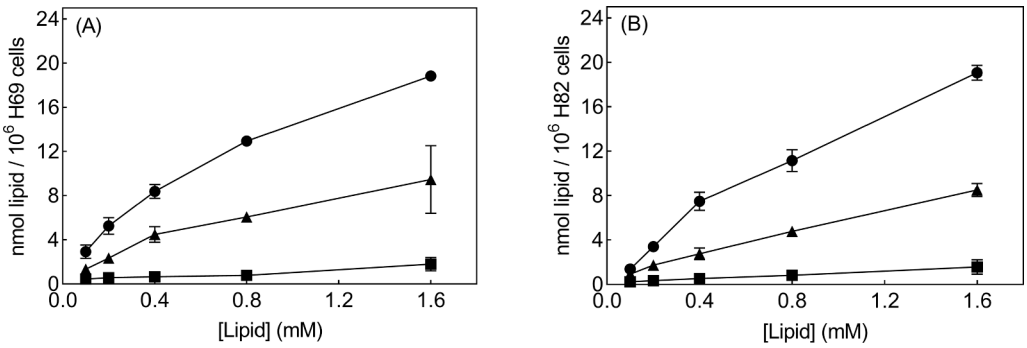


**Fig. 5. Cellular association of [$^3$H] G-SALP and non-targeted [$^3$H] SALP formulations to SCLC cells.** (A) SCLC H69 cells or (B) Variant SCLC H82 cells. SALP formulations were composed of DSPC:CHOL:DODAP:PEG-Cer$C_{16}$:Mal-PEG-DSPE at 20:45:25:8:2. Both cell lines (1 × 10$^6$ cells/well) were incubated with increasing concentrations (0.1 to 1.6 mM/well) of [$^3$H]CHE-labelled PI(G-SALP) or SALP liposomes either at 37 °C or 4 °C for 1 h. G-SALP at 37 °C, (●); G-SALP at 4 °C, (▲); SALP at 37 °C, (■). Data are expressed as nmol lipid per million cells. Results are the mean ± standard deviation of 4 samples from one representative experiment.

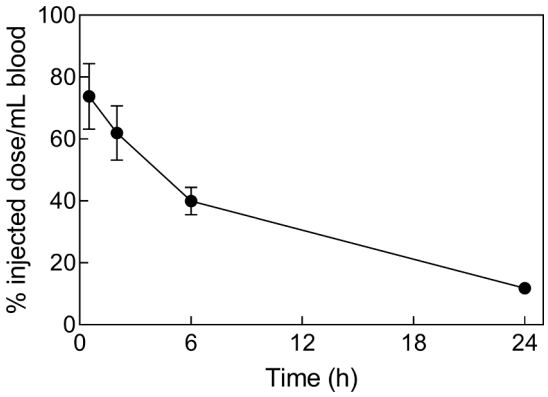


**Fig. 7. Blood profile of PI(G-SALP) in naïve BALB/c mice.** SALP liposomes composed of DSPC:CHOL:DODAP:PEG-CerC$_{16}$:Mal-PEG-DSPE at 20:45:25:8:2 M ratio, with coupled antagonist G labelled with [$^3$H]-CHE were injected i.v. in the tail vein at a single bolus dose. At different post-injection times blood was collected and digested. The resulting samples were counted for $^3$H. Data are the mean ± standard deviation of 4 animals/time point and are expressed as the percentage of injected dose per mL of blood.

increases the site-specific delivery and internalization of these lipidic DDS into their target cells (Allen et al., 2002; Fonseca et al., 2021; Iden and Allen, 2001). In this work we propose a technological platform for active targeting which can be used as a general procedure to develop peptide-targeted DDS. Depending on several factors including the physico-chemical properties of the loaded drug and the selected ligand, the preparation method and lipid bilayer characteristics, the post-insertion or direct covalent linkage approaches can be selected.

To demonstrate how this technological platform can be used, we developed antagonist G–targeted stabilized antisense lipid particles (SALP) (adapted from Semple *et al.* (Semple et al., 2001)) and LCL (adapted from (Corvo et al., 2015)). Different coupling methods for attaching ligands to the surface of liposomes have been described in the literature (Eroglu and Ibrahim, 2020; Hansen et al., 1995; Noble et al., 2004; Sawant and Torchilin, 2012). Previous work in our group has shown that for peptides and proteins the best coupling reactions involve a thiol group in the peptide and maleimide at the distal end of PEG (Vale et al., 2006). To obtain a peptide/protein-targeted liposomal formulation two approaches can be used. Either we have a liposomal formulation with a functional distal PEG, which then is used to perform the coupling reaction with the peptide, the so-called conventional coupling technique (Brignole et al., 2003; Brignole et al., 2004; Corvo et al., 2015; Corvo et al., 2016; Pagnan et al., 2000; Stuart and Allen, 2000), or we have the post-insertion technique previously developed (Iden and Allen, 2001; Ishida et al., 1999; Moreira et al., 2002; Uster et al., 1996) where the active PEG is coupled to the peptide and the resulting conjugate is post-inserted in preformed liposomes via micellar structure.

Results obtained in this work demonstrated that the amounts of drug *(as(c-myc))* loaded, and liposome size can be affected by the lipid composition and by the drug physical–chemical properties, respectively (Table 3). It must be noted that the amount of antagonist G attached at the surface of the liposomal formulations was also dependent on the coupling method and lipid composition used. As can be observed in Table 3 there was a reduction of the encapsulation parameters for both the G–SALP and PI(G–SALP) formulations when compared to SALP. This may have been caused by a destabilization in the SALP bilayer structure leading to the leakage of the encapsulated *as(c-myc)*. In the direct coupling method this destabilization in the bilayer structure was probably caused by the long (12 to 18 h) incubation time (at room temperature) needed for the covalent attachment of antagonist G to the extremity of PEG chains grafted onto SALP. In the post-insertion method bilayer destabilization was probably caused by the 1 h incubation at a high temperature (60 °C) when antagonist G–PEG–DSPE conjugate micelles should transfer onto the SALP bilayer. As both these reactions occurred at physiological pH, the ionisable amino lipid DODAP is neutral (pKa 6.6) (Maurer et al., 2001). Thus, at this point in liposome preparation, the electrostatic interactions between the *as(c–myc)* and DODAP were no longer present to retain the *as(c–myc)* molecules encapsulated in liposomes. In a parallel study by other authors differing only in the asODN molecule (Santos et al., 2010), the same conclusion was drawn for equivalent results.

Our studies showed that the amount of antagonist G at the surface of the liposomes is the key factor when considering cell association and not the methodology and lipid composition used to prepare the liposomal formulations. We were able to demonstrate a positive correlation between surface antagonist G available to cell receptors and the levels of rhodamine B fluorescence associated with cells due to possible liposomal internalization in H69 cells, especially for longer incubation periods (Fig. 1 to Fig. 4). Moreover, our results suggested very low levels of non-specific liposomal adsorption since in the absence of antagonist G there was almost no liposomal interaction with cells as shown by the low fluorescence levels. We can also extrapolate that the three-dimensional structure of the peptide remains intact after being linked to Mal-PEG-DSPE, since antagonist G is still recognized by cellular receptors, which can trigger endocytosis of the liposomes.

As a proof of concept of the influence of the presence the antagonist G at the surface of liposomes for the efficient targeting of the resulting targeted formulations, we performed *in vitro* and *in vivo* studies. By comparing the cellular association of *as(c-myc)* encapsulated antagonist G-targeted formulation PI(G–SALP) with the corresponding non-targeted formulation, we found that the presence of antagonist G promoted an increase in cellular uptake in two SCLC cell lines, when compared to the corresponding non-targeted liposomes (Fig. 5). The

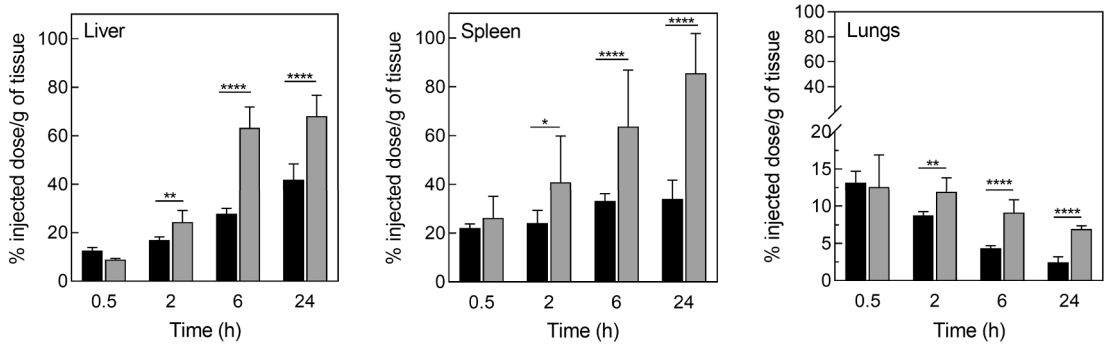


**Fig. 8. PI(G-SALP) has a higher accumulation in lungs than SALP in naïve BALB/c mice**. [3H]CHE labelled non-targeted SALP (black bars) or PI(G-SALP) (grey bars) liposomes containing as(c-myc) were injected i.v. in the tail vein at a single bolus dose. At different post-injection times liver, spleen and lungs were collected and digested. The resulting samples were counted for 3H. Data are the mean ± standard deviation of 4 animals/time point and are expressed as the percentage of injected dose per gram of tissue. *P < 0.05; **P < 0.01; ***P < 0.001; ****P < 0.0001.

results obtained demonstrate that the presence of antagonist G mediated the *in vitro* specific recognition and internalization of liposomes into the H69 and the H82 SCLC cell lines. The differences in cellular association obtained in the experiments carried out at 4 °C and 37 °C was additional evidence that antagonist G-targeted liposomes were being internalized by both cell lines. Results from the competition experiments where antagonist G coupled to LCL inhibited the binding of PI(G-SALP), provided yet further support that internalization of PI(G-SALP) was receptor-mediated. This conclusion was in agreement with previous reports (Moreira et al., 2001; Moreira et al., 2002; Santos et al., 2010) that demonstrated that antagonist G coupled to LCL either by a conventional technique, or by the post-insertion approach, led to an increased binding and internalization of antagonist G-targeted formulations into human SCLC cell lines, on a peptide- and cell-specific manner, to deliver an anti-cancer drug.

It is recognized that for targeted liposomes to gain access to tumour sites and deliver their entrapped load *in vivo*, long circulation times are required (Allen et al., 2002). The PI(G–SALP) formulation developed in this study displays a blood clearance profile similar to that of LCL (Allen and Hansen, 1991). This characteristic is provided by their small size (<120 nm) and the inclusion of DSPE-PEG in the formulation.

From the biodistribution studies we can conclude that both targeted and non–targeted SALP formulations have comparable profiles, however, the main organs of accumulation are different, the liver for SALP and spleen for PI(G-SALP). The lung also presents a reasonable value, particularly for the targeted formulation. An interesting result was the preferred spleen uptake of PI(G-SALP). The cause for this observation has not been clarified, but some specific binding of the antagonist G may be occurring in this organ. Regarding this effect, Moreira *et al.* (Moreira et al., 2001) have suggested that antagonist G may stimulate vasopressin receptor–mediated splenic uptake of antagonist G-targeted liposomes. Knowing that vasopressin receptors are expressed in the spleen (Elands et al., 1990), the observed higher PI(G–SALP) uptake is consistent with the hypothesis of an enhanced vasopressin receptor-mediated endocytosis of this formulation in the spleen. Nevertheless, what was more remarkable to observe in the biodistribution studies was the higher accumulation of the PI(G–SALP) in the lung, our organ of interest when compared to SALP liposomes. The possibility of achieving a considerable accumulation in the target organ, as demonstrated by our results, points to the need of evaluating the biodistribution studies in appropriate SCLC tumour-bearing mice.

In conclusion, the surface of different types of liposomes including a stealth mask and ligand receptor capability will determine their *in vivo* behaviour. The development of ligand-mediated targeted liposomes with long circulating properties combines the advantages of higher liposome uptake by target cells and, therefore, higher drug accumulation in target cells and prolonged circulation time. In this work we demonstrated that depending on the drug to be encapsulated, two different approaches to generate ligand-mediated targeted liposomes with higher extent of *in vitro* cell internalization can be used. We were also able to successfully generate antagonist G-targeted lipid particles with the aim of treating SCLC with high loading efficiency, high extent of *in vitro* cell internalization, and long-circulating properties *in vivo*.

## Funding

This research was funded by Fundação para a Ciência e a Tecnologia, F.C.T., I.P., through research grants UID/Multi/00612/2019, UIDB/00100/2020 and UIDP/00100/2020 grant FCT/MEC (UID/DTP/04138/2020 and UIDP/04138/2020) financing Research Institute for Medicines – iMed.ULisboa.

## CRediT authorship contribution statement

**Manuela Carvalheiro:** Conceptualization, Methodology, Formal analysis, Investigation, Data curation, Writing – original draft, Writing – review & editing. **Margarida Ferreira-Silva:** Investigation, Data curation, Writing – original draft, Writing – review & editing. **Denys Holovanchuk:** Investigation. **H. Susana Marinho:** Conceptualization, Methodology, Formal analysis, Resources, Data curation, Writing – original draft, Writing – review & editing, Visualization, Supervision, Funding acquisition. **João Nuno Moreira:** Conceptualization, Formal analysis, Writing – review & editing, Funding acquisition. **Helena Soares:** Methodology, Formal analysis, Data curation. **M. Luisa Corvo:** Conceptualization, Methodology, Formal analysis, Resources, Data curation, Writing – review & editing, Visualization, Supervision, Funding acquisition. **Maria Eugénia M. Cruz:** Conceptualization, Formal analysis, Resources, Data curation, Writing – original draft, Writing – review & editing, Visualization, Supervision, Funding acquisition.

## Declaration of Competing Interest

The authors declare that they have no known competing financial interests or personal relationships that could have appeared to influence the work reported in this paper.

## References

Allen, T.M., 2002. Ligand-targeted therapeutics in anticancer therapy. Nat. Rev. Cancer 2, 750–763.
Allen, T.M., Cullis, P.R., 2013. Liposomal drug delivery systems: from concept to clinical applications. Adv. Drug Deliv. Rev. 65, 36–48.
Allen, T.M., Hansen, C., 1991. Pharmacokinetics of stealth versus conventional liposomes: effect of dose. BBA 1068, 133–141.
Allen, T.M., Sapra, P., Moase, E., Moreira, J., Iden, D., 2002. Adventures in targeting. J. Liposome Res. 12, 5–12.
Brignole, C., Pagnan, G., Marimpietri, D., Cosimo, E., Allen, T.M., Ponzoni, M., Pastorino, F., 2003. Targeted delivery system for antisense oligonucleotides: a novel experimental strategy for neuroblastoma treatment. Cancer Lett. 197, 231–235.
Brignole, C., Pastorino, F., Marimpietri, D., Pagnan, G., Pistorio, A., Allen, T.M., Pistoia, V., Ponzoni, M., 2004. Immune cell-mediated antitumor activities of GD2-targeted liposomal c-myb antisense oligonucleotides containing CpG motifs. J. Natl Cancer Inst. 96, 1171–1180.
Chabner, B.A., Roberts Jr., T.G., 2005. Timeline: Chemotherapy and the war on cancer. Nat. Rev. Cancer 5, 65–72.
Corvo, M.L., Marinho, H.S., Marcelino, P., Lopes, R.M., Vale, C.A., Marques, C.R., Martins, L.C., Laverman, P., Storm, G., Martins, M.B., 2015. Superoxide dismutase enzymosomes: carrier capacity optimization, in vivo behaviour and therapeutic activity. Pharm. Res. 32, 91–102.
Corvo, M.L., Marinho, H.S., Martins, M.B.F., 2016. Nanomedicines as a strategy for the therapeutic use of superoxide dismutase. In: Phillips, N.H. (Ed.), Superoxide Dismutase (SOD): Sources, Therapeutics and Health Benefits. Nova Science Publisher's, Inc. - Nova Biomedical, New York, pp. 135–170.
Danhier, F., Feron, O., Preat, V., 2010. To exploit the tumor microenvironment: Passive and active tumor targeting of nanocarriers for anti-cancer drug delivery. J. Control. Release 148, 135–146.
Elands, J., Resink, A., De Kloet, E.R., 1990. Neurohypophyseal hormone receptors in the rat thymus, spleen, and lymphocytes. Endocrinology 126, 2703–2710.
Eroğlu, İ., İbrahim, M., 2020 Mar. Liposome-ligand conjugates: a review on the current state of art. J. Drug Target. 28 (3), 225–244. https://doi.org/10.1080/1061186X.2019.1648479.
Falzone, L., Salomone, S., Libra, M., 2018 Nov. Evolution of Cancer Pharmacological Treatments at the Turn of the Third Millennium. Front. Pharmacol. 13 (9), 1300. https://doi.org/10.3389/fphar.2018.01300.
Fonseca, N.A., Gregório, A.C., Mendes, V.M., Lopes, R., Abreu, T., Gonçalves, N., Manadas, B., Lacerda, M., Figueiredo, P., Pereira, M., Gaspar, M., Colelli, F., Pesce, D., Signorino, G., Focareta, L., Fucci, A., Cardile, F., Pisano, C., Cruz, T., Almeida, L., Moura, V., Simões, S., Moreira, J.N., 2021. GMP-grade nanoparticle targeted to nucleolin downregulates tumor molecular signature, blocking growth and invasion, at low systemic exposure. Nano Today 37.
Gottesman, M.M., Lavi, O., Hall, M.D., Gillet, J.P., 2016. Toward a Better Understanding of the Complexity of Cancer Drug Resistance. Annu. Rev. Pharmacol. Toxicol. 56, 85–102.
Hansen, C.B., Kao, G.Y., Moase, E.H., Zalipsky, S., Allen, T.M., 1995. Attachment of antibodies to sterically stabilized liposomes: evaluation, comparison and optimazation of coupling procedures. BBA 1239, 133–144.
Heuser, J.E., Anderson, R.G., 1989. Hypertonic media inhibit receptor-mediated endocytosis by blocking clathrin-coated pit formation. J. Cell Biol. 108, 389–400.
Iden, D.L., Allen, T.M., 2001. in vitro and in vivo comparison of immunoliposomes amde by convencional coupling techniques with those made by a new post-insertion approach. BBA 1513, 207–216.
Ishida, T., Iden, D.L., Allen, T.M., 1999. A combinatorial approach to producing sterically stabilized (Stealth) immunoliposomal drugs. FEBS Lett. 460, 129–133.

Kirpotin, D., Park, J.W., Hong, K., Zalipsky, S., Li, W.L., Carter, P., Benz, C.C., Papahadjopoulos, D., 1997. Sterically stabilized anti-HER2 immunoliposomes: design and targeting to human breast cancer cells in vitro. Biochemistry 36, 66–75.

Langdon, S., Sethi, S., Ritchie, A., Muir, M., Smyth, J., Rozengurt, E., 1992. Broad spectrum neuropeptide antagonist inhibit the growth of small cell lung cancer *in vivo*. Cancer Res. 52, 4554–4557.

MacKinnon, A.C., Armstrong, R.A., Waters, C.M., Cummings, J., Smyth, J.F., Haslett, C., Sethi, T., 1999. [Arg6, D-Trp 7,9, NmePhe8]-substance P (6–11) activates JNK and induces apoptosis in small cell lung cancer cells via an oxidant-dependent mechanism. Br. J. Cancer 80, 1026–1034.

Marcelino, P., Marinho, H.S., Campos, M.C., Neves, A.R., Real, C., Fontes, F.S., Carvalho, A., Feio, G., Martins, M.B.F., Corvo, M.L., 2017. Therapeutic activity of superoxide dismutase-containing enzymosomes on rat liver ischaemia-reperfusion injury followed by magnetic resonance microscopy. Eur. J. Pharm. Sci. 109, 464–471.

Maurer, N., Wong, K.F., Stark, H., Louie, L., McIntosh, D., Wong, T., Scherrer, P., Semple, S.C., Cullis, P.R., 2001. Spontaneous entrapment of polynucleotides upon electrostatic interaction with ethanol-destabilized cationic liposomes. Biophys. J. 80, 2310–2326.

Moreira, J.N., Gaspar, R., 2004. Antagonist G-mediated targeting and cytotoxicity of liposomal doxorubicin in NCI-H82 variant small cell lung cancer. Braz. J. Med. Biol. Res. 37, 1185–1192.

Moreira, J.N., Hansen, C.B., Gaspar, R., Allen, T.M., 2001. A growth factor antagonist as a targeting agent for sterically stabilized liposomes in human small cell lung cancer. BBA 1514, 303–317.

Moreira, J.N., Ishida, T., Gaspar, R., Allen, T.M., 2002. Use of the post-insertion technique to insert peptide ligands into pre-formed stealth liposomes with retention of binding activity and cytotoxicity. Pharm. Res. 19, 265–269.

Moura, V., Lacerda, M., Figueiredo, P., Corvo, M.L., Cruz, M.E.M., Soares, R., de Lima, M. C.P., Simoes, S., Moreira, J.N., 2012. Targeted and intracellular triggered delivery of therapeutics to cancer cells and the tumor microenvironment: impact on the treatment of breast cancer. Breast Cancer Res. Treat. 133, 61–73.

Noble, C.O., Kirpotin, D.B., Hayes, M.E., Mamot, C., Hong, K., Park, J.W., Benz, C.C., Marks, J.D., Drummond, D.C., 2004. Development of ligand-targeted liposomes for cancer therapy. Expert Opin Ther Targets 8, 335–353.

Pagnan, G., Stuart, D.D., Pastorino, F., Raffaghello, L., Montaldo, P.G., Allen, T.M., Calabretta, B., Ponzoni, M., 2000. Delivery of c-myb Antisense Oligodeoxynucleotides to Human Neuroblastoma Cells Via Disialoganglioside $GD_2$-Targeted Immunoliposomes: Antitumor Effects. J. Natl Cancer Inst. 92, 253–261.

Patra, J.K., Das, G., Fraceto, L.F., Campos, E.V.R., Rodriguez-Torres, M.D.P., Acosta-Torres, L.S., Diaz-Torres, L.A., Grillo, R., Swamy, M.K., Sharma, S., Habtemariam, S., Shin, H.S., 2018. Nano based drug delivery systems: recent developments and future prospects. J Nanobiotechnology 16, 71.

Perez-Herrero, E., Fernandez-Medarde, A., 2015. Advanced targeted therapies in cancer: Drug nanocarriers, the future of chemotherapy. Eur. J. Pharm. Biopharm.: Off. J. Arbeitsgemeinschaft fur Pharmazeutische Verfahrenstechnik e.V 93, 52–79.

Peterman, G., Spencer, C., Sperling, A., Bluestone, J., 1993. Role of gamma tau T cells in murine collagen-induced arthritis. J. Immunol. 151, 6546–6558.

Poirier, J.T., George, J., Owonikoko, T.K., Berns, A., Brambilla, E., Byers, L.A., Carbone, D., Chen, H.J., Christensen, C.L., Dive, C., Farago, A.F., Govindan, R., Hann, C., Hellmann, M.D., Horn, L., Johnson, J.E., Ju, Y.S., Kang, S., Krasnow, M., Lee, J., Lee, S.H., Lehman, J., Lok, B., Lovly, C., MacPherson, D., McFadden, D., Minna, J., Oser, M., Park, K., Park, K.S., Pommier, Y., Quaranta, V., Ready, N., Sage, J., Scagliotti, G., Sos, M.L., Sutherland, K.D., Travis, W.D., Vakoc, C.R., Wait, S. J., Wistuba, I., Wong, K.K., Zhang, H., Daigneault, J., Wiens, J., Rudin, C.M., Oliver, T.G., 2020. New Approaches to SCLC Therapy: From the Laboratory to the Clinic. J. Thorac. Oncol. 15, 520–540.

Rouser, G., Fleischer, S., Yamamoto, A., 1970. Two dimensional Thin Layer Chromatographic Separation of Polar Lipids and Determination of Phospholipids by Phosphorus Analysis of Spots. Lipids 5, 494–496.

Santos, A.O., da Silva, L.C., Bimbo, L.M., de Lima, M.C., Simoes, S., Moreira, J.N., 2010. Design of peptide-targeted liposomes containing nucleic acids. BBA 1798, 433–441.

Sawant, R.R., Torchilin, V.P., 2012. Challenges in Development of Targeted Liposomal Therapeutics. AAPS J. 14, 303–315.

Schirrmacher, V., 2019. From chemotherapy to biological therapy: A review of novel concepts to reduce the side effects of systemic cancer treatment (Review). Int. J. Oncol. 54, 407–419.

Semple, S.C., Klimuk, S.K., Harasym, T.O., dos Santos, N., Ansell, S.M., Wong, K.F., Maurer, N., Stark, H., Cullis, P.R., Hope, M.J., Scherrer, P., 2001. Effcient encapsulation of antisense oligonucleotides in lipid vesicles using ionizable aminolipids: formation of novel small multilamellar vesicle structures. BBA 1510, 152–166.

Sethi, S., Langdon, S., Smyth, J.F., Rozengurt, E., 1992. Growth of small cell lung cancer cells: stimulation by multiple neuropeptides and inhibition by broad spectrum antagonist in vitro and in vivo. Cancer Research (SUPPL.) 52, 2737s–2742s.

Stuart, D.D., Allen, T.M., 2000. A new liposomal formulation for antisense oligodeoxynucleotides with small size, high incorporation effciency and good stability. BBA 1463, 219–229.

Uster, P.S., Allen, T.M., Daniel, B.E., Mendez, C.J., Newman, M.S., Zhu, G.Z., 1996. Insertion of poly(ethylene glycol) derivatized phospholipid into pre- formed liposomes results in prolonged in vivo circulation time. FEBS Lett. 386, 243–246.

Vale, C., Corvo, M.L., Martins, L.C.D., Marques, C.R., Storm, G., Cruz, M.E.M., Martins, M.B.F., 2006. Construction of enzymosomes: optimization of coupling parameters. NSTI-Nanotech 2006, 396–397.

Yingchoncharoen, P., Kalinowski, D.S., Richardson, D.R., 2016. Lipid-Based Drug Delivery Systems in Cancer Therapy: What Is Available and What Is Yet to Come. Pharmacol. Rev. 68, 701–787.